Heterogeneous Nitrosation Reactions of Amines Driven by Dinitrogen Tetroxide: A Missing Source of Particulate Nitrosamines

Tai-Xing Chi[1,★], An Ning[2,★], Shuang Ni[1], Wei-Kang Xiao[2], Yang Liu[2], Xiu-Cong Deng[2], Ling Liu[2], Feng-Yang Bai[1,2,*], Zhen Zhao[1,3], and Xiu-Hui Zhang[2,*]

[1]Institute of Catalysis for Energy and Environment, College of Chemistry and Chemical Engineering, Shenyang Normal University, Shenyang 110034, China
[2]State Key Laboratory of Environment Characteristics and Effects for Near-space, Key Laboratory of Cluster Science, Ministry of Education of China, School of Chemistry and Chemical Engineering, Beijing Institute of Technology, Beijing 100081, China
[3]State Key Laboratory of Heavy Oil Processing, China University of Petroleum, Chang Ping, Beijing 102249, China

[★]These authors contributed equally to this work.

Correspondence to: Feng-Yang Bai (baify492@nenu.edu.cn) and Xiu-Hui Zhang (zhangxiuhui@bit.edu.cn)

ABSTRACT: Nitrosamines are carcinogenic nitrogen-containing atmospheric pollutants that are widely detected in particulate matter. However, their formation mechanisms remain poorly understood. While gas-phase and bulk aqueous pathways have been extensively investigated, the role of heterogeneous interfacial chemistry remains largely unexplored. Herein, we elucidate the molecular mechanisms underlying heterogeneous nitrosamine formation via amine-mediated reactions with dinitrogen tetroxide (N_2O_4) at the air–water interface using Born–Oppenheimer molecular dynamics and metadynamics simulations. These reactions proceed through two distinct and competing pathways: (*i*) a kinetically favored, barrierless N-nitrosation pathway in which N_2O_4 directly reacts with methylamine (MA) or dimethylamine (DMA), yielding nitrosamine cations and nitrate ions (NO_3^-); and (*ii*) a MA/DMA-mediated hydrolysis pathway of N_2O_4 that rapidly generates interfacial HONO (~2–16 ps), providing a potential secondary source of nitrosamines via subsequent HONO-mediated nitrosation with a free-energy barrier of 7.65 kcal mol^{-1} at 300 K. These findings reveal amine-mediated interfacial chemistry as an important heterogeneous pathway distinct from bulk processes, providing molecular insights into urban reactive nitrogen cycling and improving atmospheric chemical transport models.

1 Introduction

Organic nitrogen (ON) compounds constitute a pivotal yet chemically complex fraction of the global nitrogen cycle, accounting for ~30% of total atmospheric nitrogen (Cape et al., 2011). Active ON precursors play a critical role in atmospheric particle formation, with direct impacts on radiative forcing, regional climate, and public health (Finlayson-Pitts and Pitts Jr, 1999; Seinfeld and Pandis, 2016; Zhang and Anastasio, 2001). Among ON species, nitrosamines containing the N–NO functional group are of particular concern due to their potent carcinogenicity (IARC, 2007) and widespread detection in ambient particles.

Nitrosamines such as N-nitrosomethylamine (NMA) and N-nitrosodimethylamine (NDMA), which are derived from methylamine (MA) and dimethylamine (DMA) (Choi et al., 2021; Da Silva, 2013), have attracted growing attention in atmospheric chemistry and environmental health research. Notably, particulate NDMA has been detected at considerable levels (up to 20.35 ng m^{-3}) in major urban areas across Asia and Europe, including Seoul, Beijing, Urumqi, London, and Zonguldak (Akyüz and Akyüz, 2025; Choi et al., 2020, 2021, 2025a, b; Farren et al., 2015; Kim et al., 2025; Ma et al., 2025; Wang et al., 2023). However, the contribution of heterogeneous chemical processes to particulate nitrosamine formation remains poorly understood (Wang et al., 2023), limiting accurate source apportionment and effective control strategies.

Atmospheric particulate nitrosamines stem from anthropogenic primary emissions, such as vehicular exhaust, fossil fuel or biomass combustion, and industrial operations (Ge et al., 2011; Nielsen et al., 2012a, b; NTP, 2016). However, increasing evidence indicates that secondary formation via chemical reactions can also contribute substantially to ambient nitrosamine levels (Choi et al., 2020, 2021), yet the currently recognized pathways cannot fully account for the observed atmospheric concentrations. For instance, the gas-phase pathway involving reactions between amine radicals and NO followed by particle partitioning is unlikely to fully explain the observed nitrosamine abundances because nitrosamines undergo rapid atmospheric photolysis, which limits their atmospheric persistence (Nielsen et al., 2012a, b). Furthermore, aqueous-phase ozonation of amines has been explored (Choi et al., 2024; Karl et al., 2012a; Mai and Kim, 2024), but this pathway only proceeds under high ozone concentrations that are unrealistic under typical atmospheric conditions. Although amines can undergo aqueous N-nitrosation with N_2O_3, N_2O_4, and HONO (Challis and Kyrtopoulos, 1979; Choi et al., 2021, 2025a; Hutchings et al., 2010; Karl et al., 2012b), these aqueous-phase pathways have been predicted to be kinetically insufficient to explain the high particulate nitrosamine concentrations observed in the atmosphere (Choi et al., 2021; Karl et al., 2012b), suggesting the existence of an important yet unrecognized formation pathway. For N_2O_4-mediated nitrosation in particular, early mechanistic studies proposed that the asymmetric ON–ONO_2 isomer, rather than the symmetric ON–ONO_2 dimer, serves as the active nitrosating species (Challis et al., 1982; White and Feldman, 1957). This view was further corroborated by the theoretical calculations of Lv et al. (2008), who explicitly identified the asymmetric ON–ONO_2 isomer as the key intermediate responsible for NDMA formation. However, these prior theoretical investigations were all performed on isolated gas-phase molecules or using implicit-solvent models, which cannot reproduce the dynamic solvent environment and reaction kinetics of heterogeneous processes at atmospheric air–water interfaces.

These previous mechanistic studies motivate the hypothesis that the air–water interface provides a distinct reactive environment that may fundamentally alter the kinetics and molecular mechanism of N-nitrosation. This possibility is motivated not only by the inability of existing gas- and aqueous-phase pathways to explain the observed particulate nitrosamine levels, but also by accumulating evidence that MA and DMA exhibit strong interfacial propensity (Deng et al., 2026; Ning et al., 2023, 2024) and that the air–water interface can substantially accelerate a wide range of atmospheric reactions (Chen et al., 2025; Fang et al., 2025; Song et al., 2024; Xie et al., 2024; Zhang et al., 2026). In addition, N_2O_4, a key nitrosating agent, has been shown to remain at the air–water interface for approximately 100 ps before dissolving into the bulk liquid (Martins-Costa et al., 2020), making heterogeneous reactions between N_2O_4 and surface-active amines kinetically plausible. Together, these

findings suggest that heterogeneous interfacial chemistry may represent a previously overlooked atmospheric source of particulate nitrosamines. However, its kinetic feasibility, free-energy landscape, and atomistic reaction mechanism have not yet been established.

In this work, we employ Born–Oppenheimer molecular dynamics (BOMD) simulations together with well-tempered metadynamics (MetaD) calculations to investigate the heterogeneous reactions of MA and DMA with N_2O_4 at the air–water interface. Building upon previous theoretical mechanistic studies, our aim is to determine whether heterogeneous interfacial chemistry provides a kinetically viable pathway for particulate nitrosamine formation under atmospheric conditions. The simulations characterize the associated free-energy landscapes and elucidate the molecular mechanisms of heterogeneous N-nitrosation, providing molecular-level insights into the roles of amine basicity, interfacial hydrogen-bond networks, proton transfer, and steric effects in governing nitrosamine formation at atmospheric aerosol surfaces.

2 Computational Methods

2.1 Born−Oppenheimer molecular dynamics (BOMD) Simulations

The heterogeneous reaction mechanisms at the air–water interface were investigated using BOMD simulations, with enhanced sampling achieved via well-tempered metadynamics (MetaD). All simulations were performed using the CP2K 2023 software interfaced with the PLUMED 2.9.0 plugin (Bussi and Tribello, 2019; Kühne et al., 2020). The calculations of electronic structure were carried out by the QUICKSTEP module, with the Gaussian and plane wave (GPW) method and the Becke–Lee–Yang–Parr (BLYP) exchange-correlation functional (Perdew and Wang, 1992), which was supplemented with Grimme's D3 dispersion correction (Grimme et al., 2010). The DZVP-MOLOPT-SR-GTH Gaussian basis set and Goedecker–Teter–Hutter (GTH) pseudopotentials were employed to describe the valence and core electrons, respectively (Goedecker et al., 1996; Hartwigsen, 1998). The cutoff energy for the Gaussian basis set was set to 40 Ry, while that for the plane-wave basis set was 280 Ry. The *NVT* ensemble was employed, with a time step of 1.0 fs. The Nosé–Hoover thermostat (Evans and Holian, 1985) was adopted to control a constant temperature of 300 K. The simulated cell (15 Å × 15 Å × 45 Å) contained 128 water molecules, with the air–water interface defined by a vacuum region (~30 Å) above the water slab (~15 Å) along the z direction (Fig. S1). The water slab was equilibrated for 10 ps using BOMD simulations, and the temperature and potential energy profiles confirmed the achievement of statistical equilibrium (Fig. S2). The details of the collective variable (CV) are provided in the Supporting Information.

2.2 Wave Function Analysis

To gain further insights into the interfacial reaction mechanisms, the wave function analysis of key structures was performed using the Multiwfn 3.8 program (Lu and Chen, 2012), while the results were visualized by VMD 1.9.3 (Humphrey et al., 1996). Specifically, the Mayer bond order (MBO) was calculated to quantify the strength of covalent bonds within the reactant molecules (Mayer, 1983). Interaction Region Indicator (IRI) analysis was carried out to examine the strength of localized

interactions in prereactants and intermolecular noncovalent interactions within interfacial products, such as hydrogen bonds (HBs). The electron localization function (ELF) was applied to probe covalently bonded regions with high ELF values, indicative of strong electron localization.

3 Results and Discussion

3.1 Interfacial N-nitrosation reactions of MA/DMA with N_2O_4

To elucidate the heterogeneous formation pathways of nitrosamines, the reactions of MA and DMA with N_2O_4 were investigated at the air–water interface using BOMD simulations. Based on the previous studies of interfacial N_2O_4 chemistry, N_2O_4 exists as the symmetric dimer $O_2N–NO_2$, which can isomerize to the asymmetric form *t*-$ONONO_2$ (Finlayson-Pitts et al., 2003; Martins-Costa et al., 2019, 2020). Thus, *t*-$ONONO_2$ was used as the reactant to explore the heterogeneous N-nitrosation mechanisms of reactions between N_2O_4 and amines. In a three-component system consisting of *t*-$ONONO_2$, the amines (MA/DMA), and interfacial water, any two species can collide and react at the air–water interface. Three collision modes between MA/DMA and *t*-$ONONO_2$ on aqueous nanodroplet surfaces were examined (Scheme 1). Mode (*i*) corresponds to gaseous MA/DMA approaching *t*-$ONONO_2$ pre-adsorbed on the aqueous droplet surface. Mode (*ii*) describes a gaseous MA/DMA–*t*-$ONONO_2$ complex colliding with the aqueous interface. Mode (*iii*) involves gaseous *t*-$ONONO_2$ approaching MA/DMA pre-adsorbed on the aqueous surface.

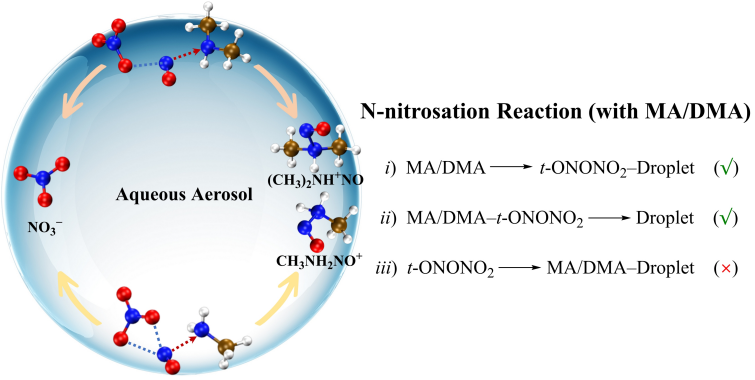

Scheme 1. Illustration of the interfacial N-nitrosation mechanism of MA/DMA initiated by *t*-$ONONO_2$ (MA/DMA + *t*-$ONONO_2$ → $CH_3NH_2NO^+/(CH_3)_2NH^+NO + NO_3^-$. The dashed lines denote ionic bonds (blue), whereas the red arrows indicate the formation of $CH_3NH_2NO^+/(CH_3)_2NH^+NO$. The yellow arrows point to the corresponding interfacial products formed in each reaction pathway. Patterns (*i*)–(*iii*) illustrate different collision scenarios, with black arrows showing the directions of collision. The blue, red, white, and ochre spheres represent the N, O, H, and C atoms, respectively. The symbols "√" and "×" denote whether the reaction can or cannot occur, respectively.

Figure 1 corresponds to mode (*i*) in Scheme 1. Initially, *t*-$ONONO_2$ was placed at the air–water interface and equilibrated for 15 ps. Analyses of temperature and potential energy confirmed that statistical equilibrium was reached at 11.5 ps (Fig. S3).

This equilibrated structure was used as the initial configuration. Notably, *t*-$ONONO_2$ underwent spontaneous heterolysis to form a stable (NO_3^-)(NO^+) ion pair at the interface by 11.5 ps, which is consistent with previous interfacial simulations by Martins-Costa et al. (2020). For the MA-involved reaction (Fig. 1(a)), MA was initially in the gas phase at t = 0 ps with negligible interactions with the aqueous surface. It rapidly approached the interfacial NO^+ ion, and by 0.99 ps, the N2 atom of MA and N1 atom of NO^+ formed a N1–N2 bond, yielding the cationic nitrosamine *c*-$CH_3NH_2NO^+$. To further understand the N-nitrosation of *t*-$ONONO_2$ with MA, electron localization function (ELF) analysis was performed for key structures. As shown in Fig. 1(b), strong electron localization within the newly formed N1–N2 bond confirms the formation of the nitrosamine and nitrate ions. Extended BOMD simulations up to 21 ps verified that the products *c*-$CH_3NH_2NO^+$ and NO_3^- remained stable at the air–water interface (Fig. 1(c)). Identical reactions from different initial conformations further support the robustness of this pathway (Fig. S4).

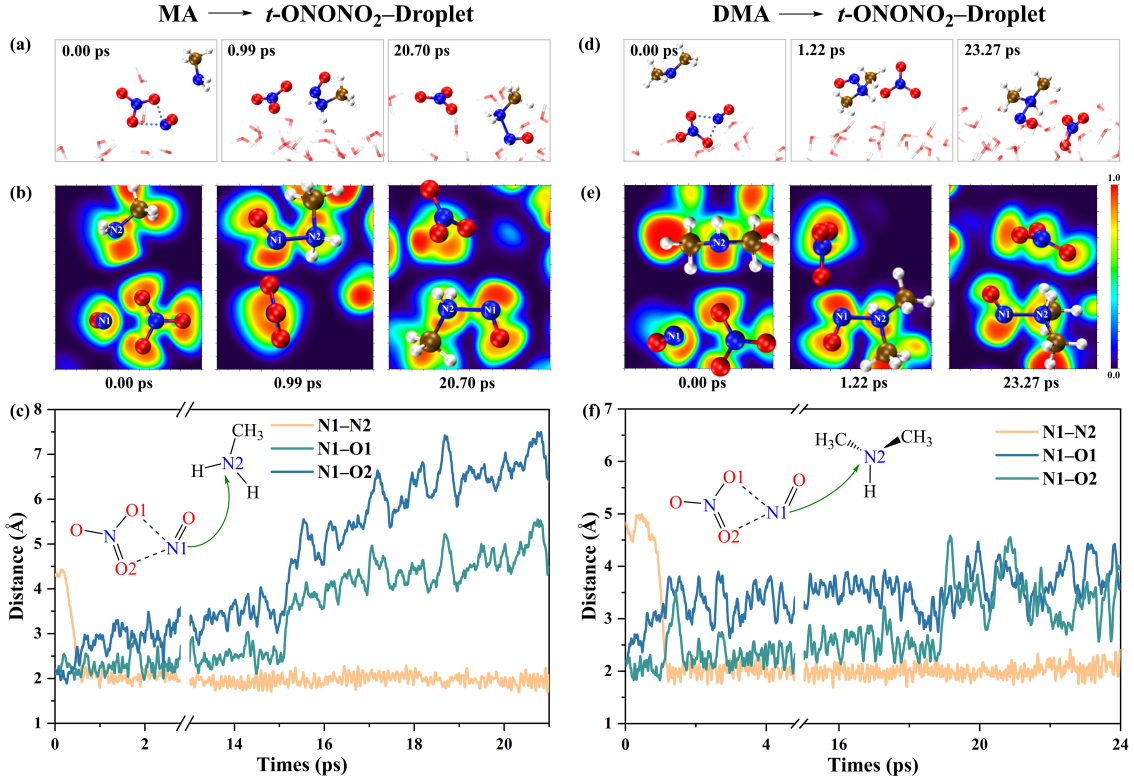

Figure 1. Snapshot structures from BOMD simulations illustrating the stepwise N-nitrosation mechanism of *t*-$ONONO_2$, the color-mapped electron localization function (ELF), and the time evolution of key bond distances mediated by MA **(a, b, c)** and DMA **(d, e, f)**. The black arrows indicate the directions of collision, while the dashed lines represent ionic bonds. The blue, red, white, and ochre spheres represent the N, O, H, and C atoms, respectively. The green arrows denote atom transfer directions.

As shown in Fig. 1(d), the DMA-mediated formation of $(CH_3)_2NHNO^+$ follows the same mechanism as that of MA. In both MA and DMA systems, nitrosamine cations form within ~1 ps and remain stable at the interface throughout the

simulations. Moreover, mode (*ii*) (Scheme 1) was also verified to be reactive. As shown in Fig. S5, the gaseous MA/DMA–*t*-$ONONO_2$ complex undergoes rapid N-nitrosation upon contacting the air–water interface, forming nitrosamine cations within 0.85 ps (MA) and 0.33 ps (DMA). These products also remain stable at the interface. Notably, mode (*iii*) did not yield direct N-nitrosation in any simulation. After equilibration, the N atom of MA/DMA formed hydrogen bonds with interfacial water, blocking the nucleophilic nitrogen site and inhibiting N-nitrosation. Interestingly, although mode (*iii*) does not produce nitrosamines directly, it efficiently promotes amine-mediated hydrolysis of *t*-$ONONO_2$ to generate HONO, protonated amine, and NO_3^-. Since HONO is also a key nitrosamine precursor, this pathway is explored in detail in a following section.

3.2 MA- and DMA-Mediated Interfacial Hydrolysis of *t*-$ONONO_2$

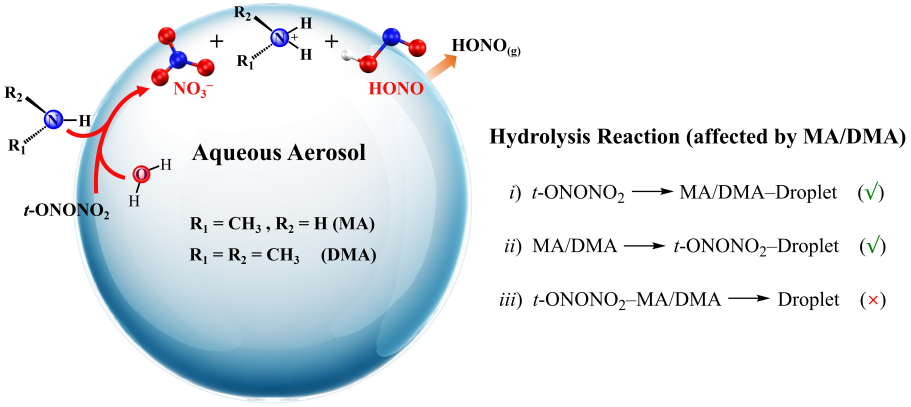

Scheme 2. Illustration of the interfacial mechanism of *t*-$ONONO_2$ hydrolysis affected by MA/DMA (*t*-$ONONO_2$ + MA/DMA + H_2O → HONO + NO_3^- + MAH^+/$DMAH^+$). Patterns (*i*)–(*iii*) illustrate different collision scenarios, with the black arrows indicating the directions of collision. The symbols "√" and "×" denote whether the reaction can or cannot occur, respectively.

We further explored the role of amines in the heterogeneous hydrolysis of *t*-$ONONO_2$. Three collision modes at the air–water interface of aqueous aerosols were investigated (Scheme 2): (*i*) gaseous *t*-$ONONO_2$ colliding with pre-adsorbed MA/DMA; (*ii*) gaseous MA/DMA approaching pre-adsorbed *t*-$ONONO_2$; (*iii*) gaseous MA/DMA–*t*-$ONONO_2$ complex adsorbing onto the water surface.

Key structures and bond-length evolutions for MA- and DMA-mediated hydrolysis corresponding to mode (*i*) are presented in Figs. 2(a)–2(d). MA was initially positioned above the water slab and equilibrated for 10 ps. Temperature and potential energy profiles confirmed equilibrium within 10 ps (Fig. S6). At equilibrium, the N atom of MA formed a hydrogen bond (HB) with interfacial water. As shown in Fig. 2(a), gaseous *t*-$ONONO_2$ does not interact with interfacial water (t = 0 ps). As the simulation proceeds, *t*-$ONONO_2$ approaches the interface and rapidly dissociates into an (NO_3^-)(NO^+) ion pair, consistent with previous reports (Martins-Costa et al., 2020) showing that this ion pair forms on the femtosecond scale and remains stable for ~100 ps at the air–water interface. Mayer bond order (MBO) and Interaction Region Indicator (IRI) analyses (Figs. S7, S8) revealed that the N2–O3 bond was the weakest, supporting this dissociation pathway. A pre-reactive complex

formed at 7.54 ps, in which interfacial water bridged the $(NO_3^-)(NO^+)$ ion pair and MA via H1–O2···N1 and O2–H1···N2 hydrogen bonds (Fig. 2(b)). Subsequently, proton H1 transfers from H_2O to MA at 8.40 ps. The resulting OH^- then attacked the N1 atom of the NO^+ ion, forming a new covalent N1–O2 bond and generating HONO by 8.48 ps. The final products are HONO, NO_3^-, and MAH^+.

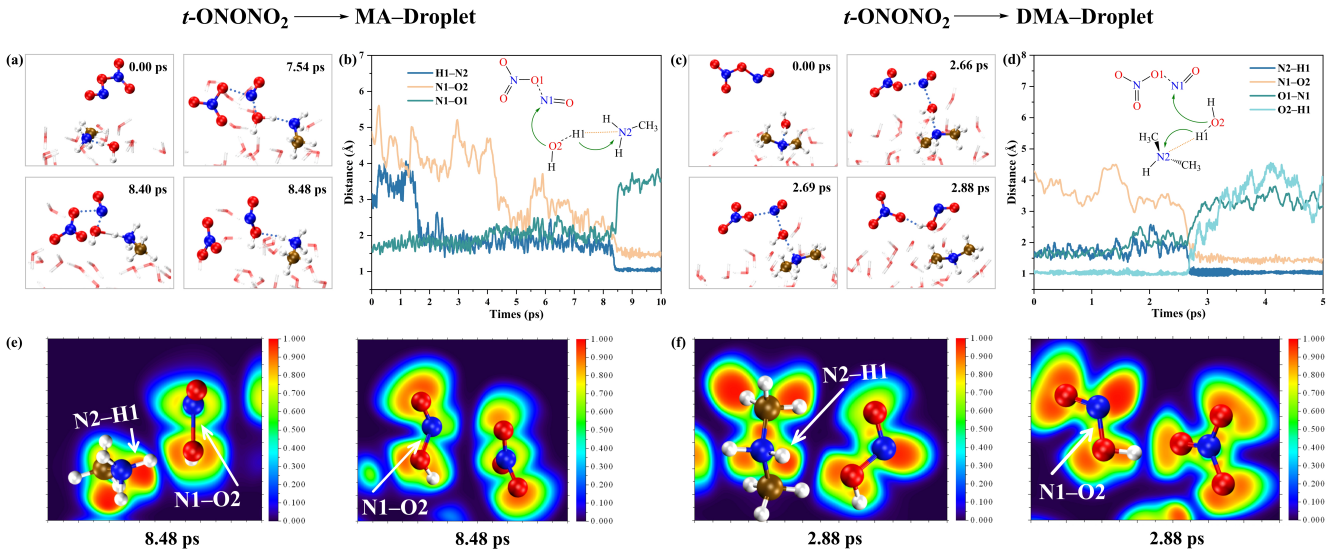

Figure 2. Snapshot structures from BOMD simulations depicting the stepwise mechanism and the time evolution of key bond distances for the hydrolysis reaction of *t*-$ONONO_2$ mediated by MA **(a, b)** and DMA **(c, d)**. Color-mapped ELF distributions for the products of MA- and DMA-mediated hydrolysis of *t*-$ONONO_2$, respectively: **(e)** HONO, MAH^+, and NO_3^- (8.48 ps); **(f)** HONO, $DMAH^+$, and NO_3^- (2.88 ps). The black arrows indicate the directions of collision, while the dashed lines represent intermolecular interactions (ionic bonds and hydrogen bonds). The blue, red, white, and ochre spheres represent the N, O, H, and C atoms, respectively. The green arrows denote atom transfer directions.

Similar to MA, DMA also initially formed a hydrogen bond with interfacial water (Fig. S9) and mediated *t*-$ONONO_2$ hydrolysis via an identical mechanism but on a shorter timescale (2.88 ps), ultimately yielding HONO, NO_3^-, and $DMAH^+$ (Figs. 2(c, d)). The faster kinetics can be attributed to the stronger basicity of DMA relative to MA, which promotes more efficient proton transfer and accelerates bond cleavage in *t*-$ONONO_2$. Furthermore, ELF analysis of the final structures (Figs. 2(e, f)) confirms clear electron localization in the N1–O2 and N2–H1 covalent bonds, as well as fully separated HONO, MAH^+, $DMAH^+$, and NO_3^-. These results demonstrate that *t*-$ONONO_2$ undergoes "single-water" hydrolysis at the aqueous interface, with only one water molecule directly participating.

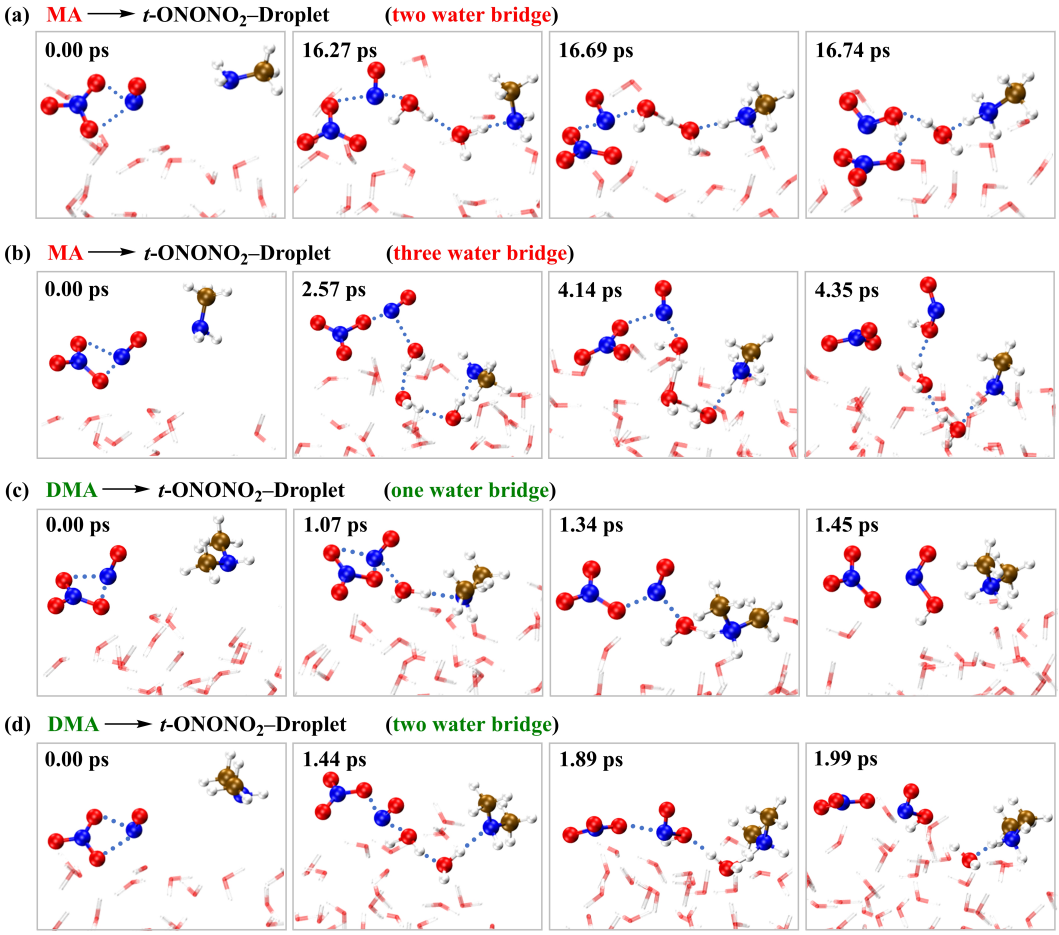

Figure 3. Snapshot structures from BOMD simulations, illustrating the stepwise mechanism of the **(a, b)** MA- and **(c, d)** DMA-mediated hydrolysis reaction of *t*-$ONONO_2$. The black arrows indicate the directions of collision, while the dashed lines represent intermolecular interactions. The blue, red, white, and ochre spheres represent the N, O, H, and C atoms, respectively.

For mode (*ii*) (Scheme 2), gaseous MA/DMA approaches pre-adsorbed *t*-$ONONO_2$. Key structures and bond-length evolutions are shown in Figs. 3 and S10. For the MA-involved reactions (Figs. 3(a) and S10(a)), MA initially resides in the gas phase without notable interactions with the interfacial water. By 16.27 ps, MA forms an O4–H2···N2 HB with H_2O. Concurrently, interfacial water connects NO^+ ion and MA via a two-water bridge (O3–H1···O4–H2), forming a pre-reactive complex. At 16.69 ps, the H2 proton transfer from H_2O to MA generates MAH^+ and OH^-, which rapidly moves toward H1 of the proximate water molecule to form another OH^-. At 16.74 ps, O3–N1 bond formation between NO^+ and second OH^- concludes the reaction, producing HONO, NO_3^-, and MAH^+ as the final products. Notably, the catalytic hydrolysis mechanism depends on the contact configuration between gaseous MA and the interface. As shown in Figs. 3(b) and S10(b), the gaseous MA approaches interfacial water, forming the O5–H3···N2 HB at 2.57 ps. Meanwhile, interfacial water connects the NO^+ ion to MA via a three-water bridge (O3–H1···O4–H2···O5–H3), forming a pre-reactive complex. Proton transfer from water to

MA occurs at 4.14 ps, followed by proton relay along the water bridge that produces OH^-. By 4.35 ps, NO^+ reacts with OH^- via O3–N1 bond formation to produce fully separated HONO, NO_3^-, and MAH^+. For MA, a pre-reactive complex forms via two-water or three-water bridges between NO^+ and MA. Proton transfer occurs along the water bridge, followed by OH^- attack on NO^+ to form HONO. Remarkably, the three-water-bridge pathway proceeds approximately four times faster than the two-water-bridge pathway. This kinetic enhancement may stem from the greater stability of the "three-water bridge" structure, whose larger spatial configuration hinders rotation at the water interface, thereby stabilizing its connections with NO^+ and MA at both ends and facilitating proton transfer.

For the DMA-involved reactions (Figs. 3(c, d) and S10(c, d)), the interfacial hydrolysis of *t*-$ONONO_2$ follows the same mechanism but proceeds even more rapidly (~1–2 ps). This acceleration is again attributed to the stronger basicity of DMA, a result consistent with collision mode (*i*). Notably, in MA-mediated hydrolysis, proton transfer through a three-water bridge occurs faster than through a two-water bridge, highlighting the catalytic advantage of increasing the length of interfacial water bridge. In contrast, DMA-mediated hydrolysis exhibits nearly identical reaction times for single-water and two-water bridges (~1–2 ps), indicating that additional water molecules provide little further kinetic enhancement. This can be attributed to the stronger basicity of DMA than MA, which enables rapid proton abstraction from interfacial water and facilitates proton transfer, thereby promoting hydrolysis.

It is worth noting that the gas-phase pre-reactive complex *t*-$ONONO_2$–MA/DMA shown in Scheme 2 (*iii*) is structurally identical to that presented in Scheme 1 (*ii*). However, when this complex collides with the air–water interface, it preferentially undergoes N-nitrosation rather than hydrolysis. This difference can be understood from the distinct elementary steps involved in the two pathways. In the N-nitrosation pathway (Scheme 1 (*ii*)), the preformed *t*-$ONONO_2$–MA/DMA complex already possesses an N···N interaction between the amine and the NO moiety of *t*-$ONONO_2$. Upon adsorption at the air–water interface, the interfacial environment facilitates the transfer of the NO group to the amine, leading to the formation of the nitrosamine cation. In contrast, the hydrolysis pathway requires nucleophilic attack by interfacial water molecules on the *t*-$ONONO_2$ moiety, accompanied by concerted solvent-assisted proton transfer. The BOMD trajectories suggest that the pre-existing N···N interaction between the amine and the NO moiety may reduce the accessibility of interfacial water molecules to the reactive site and hinder their adoption of a favorable orientation for nucleophilic attack. Consequently, the preformed gas-phase complex preferentially undergoes N-nitrosation upon collision with the air–water interface, whereas the competing hydrolysis pathway is kinetically disfavored.

Overall, MA- and DMA-catalyzed interfacial hydrolysis of *t*-$ONONO_2$ can promote aerosol growth through enhancement of hygroscopicity, owing to the formation of (*i*) nitrate (NO_3^-) and (*ii*) protonated amines (MAH^+ and $DMAH^+$), which substantially increase aerosol water uptake (Deng et al., 2026; Ning et al., 2023, 2024). The MA- and DMA-mediated hydrolysis of *t*-$ONONO_2$ proceeds on the picosecond timescale and efficiently produces HONO. This high HONO yield is governed by the synergistic coupling between interfacial water bridges and amine basicity, which facilitate proton transfer.

Given the high reactivity of HONO, its kinetic behavior warrants investigation at the air–water interface. As shown in Fig. S11, IRI analysis reveals weak noncovalent interactions between HONO and interfacial water, supporting the finding by

Chen et al. (2025) that HONO predominantly exists in its neutral form at the interface of aqueous microdroplets. More importantly, HONO is recognized as a key precursor to N-nitrosodimethylamine (NDMA) (Ge et al., 2011; Karl et al., 2012b), despite its relatively slow bimolecular reaction rate with DMA in the aqueous phase (~0.1 M^{-1} s^{-1}) (Karl et al., 2012b). However, the heterogeneous reaction mechanism of HONO with DMA at the air–water interface remains poorly understood, yet its elucidation is essential to assess their contribution to particulate nitrosamine formation.

3.3 Interfacial Reaction of DMA with HONO

To evaluate the contribution of interfacially generated HONO to particulate-phase nitrosamine formation, we investigated the reaction of DMA with HONO at the air–water interface using BOMD and MetaD simulations. DMA was selected as the representative amine due to the substantially higher atmospheric abundance of NDMA compared to NMA in field observations, as well as the extensive data available for DMA-driven nitrosamine formation in kinetic models (Karl et al., 2012b; Choi et al., 2021, 2025a). Consequently, while MA is also a relevant precursor, the current study focuses specifically on the DMA system to align with these dominant atmospheric observations. As shown in Figs. 4(a, b), HONO first undergoes N–O bond cleavage to form an OH^-/NO^+ ion pair. Concurrently, the N–H bond of DMA dissociates; the released proton (H^+) neutralizes OH^- to form an H_2O molecule, while electrophilic NO^+ attacks $(CH_3)_2N^-$ to yield NDMA. The calculated energy barrier for this process is 7.65 kcal mol^{-1} (Fig. 4c), corresponding to an interfacial rate constant of 1.67×10^7 M^{-1} s^{-1} at 300 K based on transition state theory (TST). Computational details are provided in Section S4 of the Supporting Information. Although HONO-mediated nitrosation is kinetically feasible at the air–water interface, it is predicted to be less efficient than the direct N_2O_4-mediated pathway under the conditions investigated in this work. However, previous atmospheric kinetic models have also identified N_2O_3 as a potentially important nitrosating agent, in addition to HONO and N_2O_4. The N_2O_3-mediated pathway was not considered in the present study because, under typical nighttime atmospheric conditions, N_2O_4 is generally expected to be substantially more abundant than N_2O_3. This difference is attributed to the rapid consumption of NO by ozone, which suppresses N_2O_3 formation, whereas NO_2 readily undergoes dimerization to form N_2O_4 (Brown and Stutz, 2012; Roscoe and Hind, 1993). Nevertheless, N_2O_3-mediated interfacial nitrosation may also contribute under conditions where sufficient N_2O_3 is available. Further studies on N_2O_3-mediated interfacial reactions are therefore needed to evaluate their potential role in atmospheric nitrosamine formation.

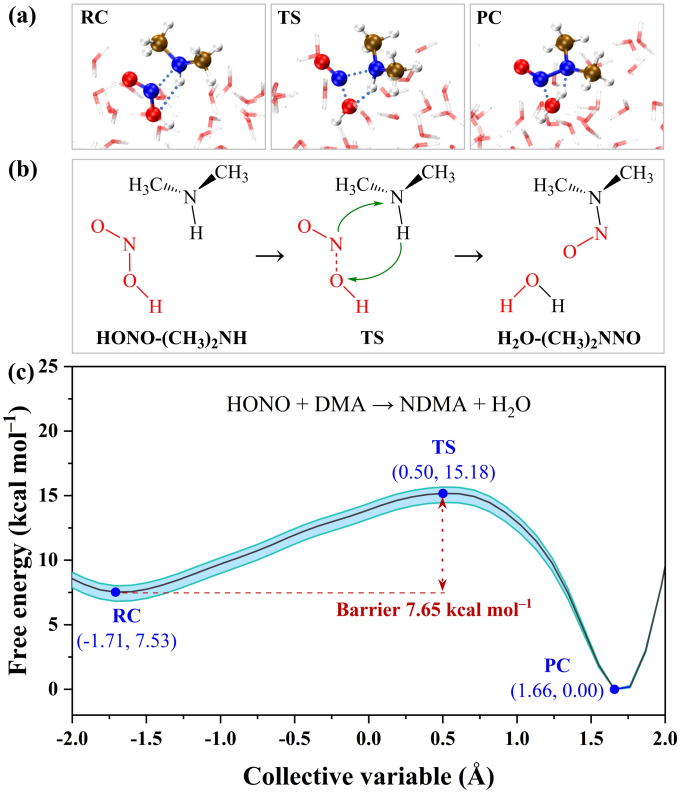

Figure 4. Direct interfacial N-nitrosation of DMA by HONO at the air-water interface. **(a)** Snapshots of the reactant complex (RC), transition state (TS), and product complex (PC) during the WT-MetaD simulations; **(b)** Reaction mechanism for DMA + HONO → NDMA + H_2O. **(c)** Free energy profile along the collective variable (black line) for the N-nitrosation process with the error band (blue region). The dashed lines represent intermolecular interactions, while the green arrows denote atom transfer directions.

Although the HONO-mediated nitrosation pathway is kinetically less favorable than the direct N-nitrosation by N_2O_4 under the investigated conditions, this pathway may become environmentally relevant under specific atmospheric scenarios. In particular, aged aerosols with prolonged atmospheric residence times and nighttime HONO-rich environments may provide favorable conditions for this secondary pathway, because heterogeneous HONO production and accumulation can increase the availability of HONO at aqueous aerosol surfaces, whereas the concentration of highly reactive N_2O_4 may decrease during aerosol evolution. Under such conditions, interfacial HONO may serve as an important reactive nitrogen reservoir, linking inorganic nitrogen species with particulate organic nitrogen formation through subsequent reactions with amines. Therefore, the HONO-mediated pathway should not be considered merely as a kinetically minor reaction, but rather as a potentially important complementary pathway that contributes to particulate nitrosamine formation under specific atmospheric conditions.

Considering that both the HONO- and N_2O_4-mediated pathways originate from reactive nitrogen species in the atmosphere, their relative importance should be evaluated within the broader context of previous molecular studies, particle-phase observations, and atmospheric kinetic models. Previous theoretical studies have provided important insights into the

intrinsic reactivity of DMA toward N_2O_4. Lv et al. (2008) systematically investigated the nitration and nitrosation pathways of DMA with N_2O_4 and identified asymmetric ON–ONO_2 as the key reactive isomer responsible for N-nitrosation. Their calculations demonstrated that ON–ONO_2 can undergo a nearly barrierless concerted reaction with DMA in both the gas phase and an implicit aqueous environment, establishing the molecular feasibility of N_2O_4-mediated nitrosamine formation. These findings provided a mechanistic basis for understanding the role of N_2O_4 as an effective nitrosating agent in aqueous environments.

Beyond these theoretical investigations, recent experimental studies have demonstrated that amines in the particulate phase can undergo heterogeneous reactions with reactive nitrogen species under atmospheric conditions. Chen et al. (2022) investigated the transformation of particulate DMA under NO_x exposure and reported the formation of both nitramine and nitrosamine products through experimental measurements and theoretical analysis. They further suggested that reactive nitrogen oxide species, including N_2O_4 and N_2O_3, may contribute to DMA transformation through interactions with the nitrogen center of the amine. However, the specific reactive intermediates and molecular pathways controlling N_2O_4-driven nitrosation at the air–water interface of aqueous aerosols remain poorly constrained.

Building upon these theoretical insights and atmospheric observations, the present study reveals how the air–water interface regulates N_2O_4-mediated nitrosation under realistic heterogeneous conditions. Consistent with the findings of Lv et al. (2008), our BOMD simulations identify *t*-$ONONO_2$ as the active nitrosating species. However, unlike what is captured in previous gas-phase and continuum-solvent models, the explicit aqueous interface introduces dynamic solvent organization, interfacial hydrogen-bond networks, and adsorption-dependent collision configurations that regulate the reaction pathway. Therefore, this work extends previous descriptions of N_2O_4-mediated nitrosation from intrinsic molecular reactivity to heterogeneous atmospheric chemistry by demonstrating that aqueous aerosol interfaces can facilitate nitrosamine formation through interface-mediated reaction dynamics.

The atmospheric implications of the proposed mechanism can be further considered in the context of existing kinetic models. Previous atmospheric chemistry models, including the SINTEF mechanism developed by Karl et al. (2012b) and the box-model study of Choi et al. (2021, 2025a), represented DMA nitrosation by HONO, N_2O_3, and N_2O_4 using parameterized reaction pathways and effective rate coefficients. Although these mechanisms provide an important framework for evaluating secondary nitrosamine formation, the associated kinetic parameters remain subject to uncertainty. Importantly, the box models developed by Choi et al. (2021, 2025a) did not incorporate heterogeneous reactions, primarily due to the limited kinetic data available at the time. Consequently, aerosol interfacial nitrosation pathways remain absent from current atmospheric kinetic models, despite their potential atmospheric relevance. Furthermore, the molecular mechanisms underlying N_2O_4-mediated nitrosation, particularly at the air–water interface of aqueous aerosols, remain poorly understood. As a result, many of the kinetic parameters adopted in current atmospheric models are based on indirect estimates, analogous systems, or empirical parameterizations rather than explicit molecular-level reaction mechanisms.

Moreover, the interfacial pathway identified in this study exhibits rapid kinetics, with the N_2O_4-mediated reaction producing nitrosamine cations within picoseconds, while the HONO-mediated interfacial pathway also proceeds efficiently.

Although the quantitative influence of this interfacial pathway on atmospheric nitrosamine budgets requires future model implementation, our findings highlight the need to incorporate aerosol interfacial chemistry into future parameterizations of heterogeneous nitrosamine formation.

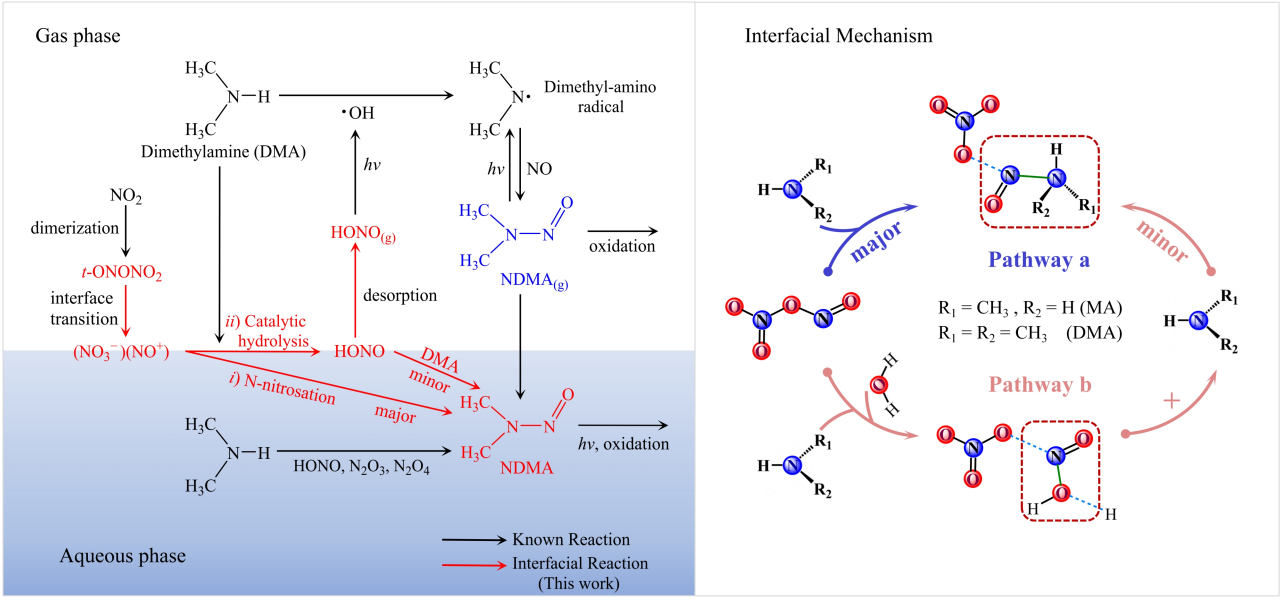

Figure 5. Schematic illustration of simplified reactive nitrogen chemistry. Black arrows represent the established gas-phase or aqueous-phase reaction pathways, whereas red arrows indicate the revealed amine-mediated heterogeneous reactions occurring at the air–water interface of aqueous aerosols. The right panel shows the detailed interfacial reaction pathway.

4 Conclusions

Particulate nitrosamines are carcinogenic organic nitrogen compounds of growing concern, yet their formation remains poorly understood, which limits accurate assessments of their impacts on air quality, climate, public health, and reactive nitrogen cycling. Particulate nitrosamines have been frequently detected at high concentrations in atmospheric particles across multiple cities in Asia and Europe. However, existing sources cannot fully account for these levels, indicating the presence of missing nitrosamine sources. To investigate these unknown origins, we employed Born-Oppenheimer molecular dynamics (BOMD) and metadynamics (MetaD) simulations to explore the heterogeneous reaction processes of MA/DMA with N_2O_4 (nitrosamine precursors) at the air–water interface of aqueous aerosols. The results demonstrate that spontaneous direct nitrosation of MA/DMA with N_2O_4 at the air–water interface provides a kinetically favorable pathway for particulate-phase nitrosamine formation. Additionally, MA/DMA can catalyze the spontaneous hydrolysis of N_2O_4 to generate HONO at the air-water interface. The subsequent reaction of HONO with DMA to form the nitrosamine NDMA, by overcoming a free energy barrier of 7.65 kcal mol^{-1}, represents a secondary formation pathway at the interface. These findings carry important environmental implications: (*i*) the nitrosamines formed at the interface increase the carcinogenic potential of atmospheric particulate matter,

thus posing heightened risks to human health; (*ii*) the formed HONO can undergo photolysis to produce ·OH radicals, which can enhance the tropospheric oxidation capacity and promote the formation of secondary pollutants. Meanwhile, these reactions concurrently generate NO_3^-, contributing to the aerosol nitrate burden. Furthermore, the NO released from the photolysis of HONO and nitrosamines can re-enter the NO_x cycle. Importantly, the coupled formation of nitrosamines, HONO, and nitrate simultaneously influences particulate toxicity, atmospheric oxidation capacity, aerosol nitrate burden, and reactive nitrogen cycling, thereby extending the atmospheric significance of the identified interfacial chemistry beyond nitrosamine formation alone. This mechanism provides a consistent molecular explanation for the frequently observed high nitrosamine levels in cloud water, fog, and urban $PM_{2.5}$. Furthermore, the identified heterogeneous interfacial N-nitrosation pathway represents a previously overlooked source of particulate nitrosamines and may account for the missing sources inferred from atmospheric observations. By incorporating the revealed interfacial N-nitrosation pathway into the established scheme of gas- and aqueous-phase nitrogen chemistry, this study advances and broadens our current understanding of multiphase reactive nitrogen cycling (Fig. 5). Incorporating this heterogeneous interfacial chemistry into atmospheric chemical transport models may improve predictions of particulate toxicity, nitrogen chemistry and budgets. More broadly, by converting gaseous reactive nitrogen into particulate nitrogen, these findings underscore the key role of heterogeneous interfacial chemistry in shaping the global nitrogen cycle.

Data availability. The data in this article are available from the corresponding author upon reasonable request (baify492@nenu.edu.cn and zhangxiuhui@bit.edu.cn).

Supplement. The supplement related to this article is available online at:

Author contribution. ⋆TC and ⋆AN contributed equally to this work. XZ, ZZ, and FB designed and supervised the research. TC, XD, and AN performed the quantum chemical calculations and the BOMD simulations. TC, AN, SN, WX, YL and LL analyzed data. TC, AN, FB, and XZ wrote the paper with contributions from all the other co-authors.

Competing interests. The contact author has declared that neither they nor their co-authors have any competing interests.

Disclaimer. Publisher's note: Copernicus Publications remains neutral with regard to jurisdictional claims in published maps and institutional affiliations.

Financial support. This work was financially supported by the National Natural Science Foundation of China (No. 22476134 and 22306011), the National Science Foundation for Distinguished Young Scholars (No. 22225607), and the Central

Government Guided Local Science and Technology Development Fund (No. 2026JH6/101000020) under the "Free Exploration Program for Young Scientists (Liaoning Provincial Youth B), and Liaoning Xingliao talented youth Top talent program (XLYC2503035). Feng-Yang Bai was also supported by the China Postdoctoral Science Foundation (No. 2024M754098).

References

Akyüz, B. G. and Akyüz, M.: Seasonal variations, source apportionment, and health risk assessment of nitrosamines in inhalable particulate matter (PM_{10}) in the atmosphere of Zonguldak, Türkiye, Environ. Sci. Pollut. Res., 32, 11083–11096, https://doi.org/10.1007/s11356-025-36280-z, 2025.

Brown, S. S. and Stutz, J.: Nighttime radical observations and chemistry, Chem. Soc. Rev., 41, 6405–6447, https://doi.org/10.1039/c2cs35181a, 2012.

Bussi, G. and Tribello, G. A.: Analyzing and Biasing Simulations with PLUMED, in: Biomolecular Simulations: Methods and Protocols, edited by: Bonomi, M. and Camilloni, C., Springer, New York, NY, 529–578, https://doi.org/10.1007/978-1-4939-9608-7_21, 2019.

Cape, J. N., Cornell, S. E., Jickells, T. D., and Nemitz, E.: Organic nitrogen in the atmosphere — Where does it come from? A review of sources and methods, Atmos. Res., 102, 30–48, https://doi.org/10.1016/j.atmosres.2011.07.009, 2011.

Challis, B. C. and Kyrtopoulos, S. A.: The chemistry of nitrosocompounds. Part 11. Nitrosation of amines by the two-phase interaction of amines in solution with gaseous oxides of nitrogen. J. Chem. Soc., Perkin Trans. 1, 299–304, https://doi.org/10.1039/P19790000299, 1979.

Challis, B. C., Shuker, D. E., Fine, D. H., Goff, E. U., and Hoffman, G. A.: Amine nitration and nitrosation by gaseous nitrogen dioxide, IARC Scientific Publication, 41, 11–20, 1982.

Chen, T., Ge, Y., Liu, Y., and He, H.: N-nitration of secondary aliphatic amines in the particle phase, Chemosphere, 293, 133639, https://doi.org/10.1016/j.chemosphere.2022.133639, 2022.

Chen, H., Yuan, X., Zhang, J., Chen, X., Francisco, J. S., Meng, Y., and Zhang, X.: Simultaneous Reduction and Oxidation of NO_2 on Water Microdroplets Provides Previously Unknown Pathways to the Formation of HONO and HNO_3, J. Am. Chem. Soc., 147, 38500–38507, https://doi.org/10.1021/jacs.5c12051, 2025.

Chen, X., Wan, Z., Bai, Q., Zhu, C., and Francisco, J. S.: HOCl/$ClONO_2$ Catalytic Cycle: Promotion of the Reactive Uptake of N_2O_5 at the Air–Water Interface, J. Am. Chem. Soc., 147, 29215–29222, https://doi.org/10.1021/jacs.5c08347, 2025.

Choi, N. R., Ahn, Y. G., Lee, J. Y., Kim, E., Kim, S., Park, S. M., Song, I. H., and Kim, Y. P.: Winter-time particulate nitrosamines and nitramines in the atmosphere at seoul, South Korea, Atmos. Environ., 237, 117582, https://doi.org/10.1016/j.atmosenv.2020.117582, 2020.

Choi, N. R., Ahn, Y. G., Lee, J. Y., Kim, E., Kim, S., Park, S. M., Song, I. H., Shin, H. J., and Kim, Y. P.: Particulate Nitrosamines and Nitramines in Seoul and Their Major Sources: Primary Emission versus Secondary Formation, Environ. Sci. Technol., 55, 7841–7849, https://doi.org/10.1021/acs.est.1c01503, 2021.

Choi, N. R., Kim, Y. P., Lee, J. Y., Kim, E., Kim, S., and Shin, H. J.: Impact of ozonation on the formation of particulate nitrosodi-methylamine (NDMA) in atmosphere, Chemosphere, 349, 140794, https://doi.org/10.1016/j.chemosphere.2023.140794, 2024.

Choi, N. R., Kim, Y. P., Lee, J. Y., Ahn, Y. G., Kim, E., Kim, S., and Shin, H. J.: Characteristics of the atmospheric behavior of particulate Nitro(so) compounds in the urban atmosphere of Seoul during Spring 2019: Role of the oxides of nitrogen to the formation of Nitro(so) compounds, Atmos. Environ., 358, 121337, https://doi.org/10.1016/j.atmosenv.2025.121337, 2025a.

Choi, N. R., Kim, Y. P., Ahn, Y. G., Lee, J. Y., Kim, E., Kim, S., and Shin, H. J.: Trend and health risk of carcinogenic particulate nitrosamines in the atmosphere in Seoul, South Korea, Atmos. Environ., 356, 121309, https://doi.org/10.1016/j.atmosenv.2025.121309, 2025b.

Da Silva, G.: Formation of Nitrosamines and Alkyldiazohydroxides in the Gas Phase: The CH_3NH + NO Reaction Revisited, Environ. Sci. Technol., 47, 7766–7772, https://doi.org/10.1021/es401591n, 2013.

Deng, X., Ning, A., Liu, L., Bai, F., Yang, J., Li, J., Liu, J., and Zhang, X.: Mechanistic insights into I_2O_5 heterogeneous hydrolysis and its role in iodine aerosol growth in pristine and polluted atmospheres, Atmos. Chem. Phys., 26, 477–488, https://doi.org/10.5194/acp-26-477-2026, 2026.

Evans, D. J. and Holian, B. L.: The Nose–Hoover thermostat, J. Chem. Phys., 83, 4069–4074, https://doi.org/10.1063/1.449071, 1985.

Fang, Y., Li, X., Yuan, C., Li, X., Yuan, X., Zhang, D., Zhang, X., Zhu, C., and Fang, W.: Spontaneous Generation of Alkoxide Radical from Alcohols on Microdroplets Surface, Angewandte Chemie, 137, e202417920, https://doi.org/10.1002/ange.202417920, 2025.

Farren, N. J., Ramírez, N., Lee, J. D., Finessi, E., Lewis, A. C., and Hamilton, J. F.: Estimated Exposure Risks from Carcinogenic Nitrosamines in Urban Airborne Particulate Matter, Environ. Sci. Technol., 49, 9648–9656, https://doi.org/10.1021/acs.est.5b01620, 2015.

Finlayson-Pitts, B. J. and Pitts Jr, J. N.: Chemistry of the Upper and Lower Atmosphere: Theory, Experiments, and Applications. Elsevier., 1999.

Finlayson-Pitts, B. J., Wingen, L. M., Sumner, A. L., Syomin, D., and Ramazan, K. A.: The heterogeneous hydrolysis of NO_2 in laboratory systems and in outdoor and indoor atmospheres: An integrated mechanism, Phys. Chem. Chem. Phys., 5, 223–242, https://doi.org/10.1039/B208564J, 2003.

Ge, X., Wexler, A. S., and Clegg, S. L.: Atmospheric amines – Part I. A review, Atmos. Environ., 45, 524–546, https://doi.org/10.1016/j.atmosenv.2010.10.012, 2011.

Goedecker, S., Teter, M., and Hutter, J.: Separable dual-space Gaussian pseudopotentials, Phys. Rev. B, 54, 1703–1710, https://doi.org/10.1103/PhysRevB.54.1703, 1996.

Grimme, S., Antony, J., Ehrlich, S., and Krieg, H.: A consistent and accurate ab initio parametrization of density functional dispersion correction (DFT-D) for the 94 elements H-Pu, J. Chem. Phys., 132, 154104, https://doi.org/10.1063/1.3382344, 2010.

Hartwigsen, C.: Relativistic separable dual-space Gaussian pseudopotentials from H to Rn, Phys. Rev. B, 58, 3641–3662, https://doi.org/10.1103/PhysRevB.58.3641, 1998.

Humphrey, W., Dalke, A., and Schulten, K.: VMD: Visual molecular dynamics, J. Mol. Graph., 14, 33–38, https://doi.org/10.1016/0263-7855(96)00018-5, 1996.

Hutchings, J. W., Ervens, B., Straub, D., and Herckes, P.: N-Nitrosodimethylamine Occurrence, Formation and Cycling in Clouds and Fogs, Environ. Sci. Technol., 44, 8128–8133, https://doi.org/10.1021/es101698q, 2010.

IARC: Smokeless Tobacco and Some Tobacco-specific N-Nitrosamines, IARC Monographs on the Evaluation of Carcinogenic Risks to Humans, Vol. 89, International Agency for Research on Cancer, Lyon, France, 2007.

Karl, M., Herckes, P., Mitch, W., and da Silva, E. F.: Atmospheric Chemistry-Aqueous phase chemistry. Sintef report, (F23082), 25-05, 2012a.

Karl, M., Herckes, P., Mitch, W., and da Silva, E. F.: SINTEF Materials and Chemistry Process Technology Atmospheric Chemistry-Aqueous phase chemistry Project 257430193: D6 Final report, 2012b.

Kim, J. Y., Kim, Y. P., Yu, X., Yu, J., Wu, Z., Lee, H.-M., Song, M., Jang, K. S., Kim, C., Choi, N. R., and Lee, J. Y.: Concentrations and formation pathways of nitrogen-containing organic compounds in $PM_{2.5}$ from Seoul and Beijing, Environ. Res., 286, 122959, https://doi.org/10.1016/j.envres.2025.122959, 2025.

Kühne, T. D., Iannuzzi, M., Del Ben, M., Rybkin, V. V., Seewald, P., Stein, F., Laino, T., Khaliullin, R. Z., Schütt, O., Schiffmann, F., Golze, D., Wilhelm, J., Chulkov, S., Bani-Hashemian, M. H., Weber, V., Borštnik, U., Taillefumier, M., Jakobovits, A. S., Lazzaro, A., Pabst, H., Müller, T., Schade, R., Guidon, M., Andermatt, S., Holmberg, N., Schenter, G. K., Hehn, A., Bussy, A., Belleflamme, F., Tabacchi, G., Glöß, A., Lass, M., Bethune, I., Mundy, C. J., Plessl, C., Watkins, M., VandeVondele, J., Krack, M., and Hutter, J.: CP2K: An electronic structure and molecular dynamics software package - Quickstep: Efficient and accurate electronic structure calculations, J. Chem. Phys., 152, 194103, https://doi.org/10.1063/5.0007045, 2020.

Lu, T. and Chen, F.: Multiwfn: A multifunctional wavefunction analyzer, J Comput Chem, 33, 580–592, https://doi.org/10.1002/jcc.22885, 2012.

Lv, C. L., Liu, Y. D., and Zhong, R.: Theoretical Investigation of Nitration and Nitrosation of Dimethylamine by N_2O_4, J. Phys. Chem. A, 112, 7098–7105, https://doi.org/10.1021/jp8029924, 2008.

Ma, J., Qi, Y., Han, Y., Ge, J., Wen, L., Fu, X., Hu, W., Shi, Z., Volmer, D. A., and Fu, P.: Sources and potential health indicators in urban aerosols revealed by gas chromatography-mass spectrometry combined with nitrogen

chemiluminescence detector: evidence from a megacity (Tianjin) of China, Atmos. Environ., 358, 121345, https://doi.org/10.1016/j.atmosenv.2025.121345, 2025.

Mai, T. T. H. and Kim, H.: Occurrence of N-nitrosamines in the atmosphere and human health risk: A case study in an urban area of Chuncheon, Gangwon State, South Korea, Environ. Pollut., 349, 123802, https://doi.org/10.1016/j.envpol.2024.123802, 2024.

Martins-Costa, M. T. C., Anglada, J. M., Francisco, J. S., and Ruiz-López, M. F.: Theoretical Investigation of the Photoexcited NO_2 +H_2O reaction at the Air–Water Interface and Its Atmospheric Implications, Chem. Eur. J., 25, 13899–13904, https://doi.org/10.1002/chem.201902769, 2019.

Martins-Costa, M. T. C., Anglada, J. M., Francisco, J. S., and Ruiz-López, M. F.: The Aqueous Surface as an Efficient Transient Stop for the Reactivity of Gaseous NO_2 in Liquid Water, J. Am. Chem. Soc., 142, 20937–20941, https://doi.org/10.1021/jacs.0c10364, 2020.

Mayer, I.: Charge, bond order and valence in the AB initio SCF theory, Chem. Phys. Lett., 97, 270–274, https://doi.org/10.1016/0009-2614(83)80005-0, 1983.

Nielsen, C. J., Herrmann, H., and Weller, C.: Atmospheric chemistry and environmental impact of the use of amines in carbon capture and storage (CCS), Chem. Soc. Rev., 41, 6684, https://doi.org/10.1039/c2cs35059a, 2012a.

Nielsen, C. J., Bossi, R., Bunkan, A. J. C., Dithmer, L., Glasius, M., Hallquist, M., Hansen, A. M. K., Lutz, A., Salo, K., and Maguta, M. M.: Atmospheric Degradation of Amines (ADA): Summary Report from Atmospheric Chemistry Studies of Amines, Nitrosamines, Nitramines and Amides, 2012b.

Ning, A., Zhong, J., Li, L., Li, H., Liu, J., Liu, L., Liang, Y., Li, J., Zhang, X., Francisco, J. S., and He, H.: Chemical Implications of Rapid Reactive Absorption of I_2O_4 at the Air-Water Interface, J. Am. Chem. Soc., 145, 10817–10825, https://doi.org/10.1021/jacs.3c01862, 2023.

Ning, A., Li, J., Du, L., Yang, X., Liu, J., Yang, Z., Zhong, J., Saiz-Lopez, A., Liu, L., Francisco, J. S., and Zhang, X.: Heterogenous Chemistry of I_2O_3 as a Critical Step in Iodine Cycling, J. Am. Chem. Soc., 146, 33229–33238, https://doi.org/10.1021/jacs.4c13060, 2024.

NTP, 2016. In: Program, N. T. (Ed.), 14th Report on Carcinogens (Roc), National Toxicology Program (NTP). US Department of Health and Human Services.

Perdew, J. P. and Wang, Y.: Accurate and simple analytic representation of the electron-gas correlation energy, Phys. Rev. B, 45, 13244–13249, https://doi.org/10.1103/PhysRevB.45.13244, 1992.

Roscoe, H. K., Hind, A. K: The equilibrium constant of NO_2 with N_2O_4 and the temperature dependence of the visible spectrum of NO_2: A critical review and the implications for measurements of NO_2 in the polar stratosphere, J. Atmos. Chem. 16, 257–276. https://doi.org/10.1007/BF00696899, 1993.

Seinfeld, J. H. and Pandis, S. N.: Atmospheric Chemistry and Physics: From Air Pollution to Climate Change; John Wiley & Sons, 2016.

Song, Z., Zhu, C., Gong, K., Wang, R., Zhang, J., Zhao, S., Li, Z., Zhang, X., and Xie, J.: Deciphering the Microdroplet Acceleration Factors of Aza-Michael Addition Reactions, J. Am. Chem. Soc., 146, 10963–10972, https://doi.org/10.1021/jacs.4c02312, 2024.

Wang, J., Zhou, X., Hua, Z., Jiang, N., and He, X.: Concentration level, health risk assessment and source apportionment of nitrosamines in $PM_{2.5}$ in Urumqi during winter time, Atmos. Pollut. Res., 14, 101756, https://doi.org/10.1016/j.apr.2023.101756, 2023.

White, E. H. and Feldman, W. R.: THE NITROSATION AND NITRATION OF AMINES AND ALCOHOLS WITH NITROGEN TETROXIDE, J. Am. Chem. Soc., 79, 5832–5833, https://doi.org/10.1021/ja01578a074, 1957.

Xie, R., Guo, K., Li, Y., Zhang, Y., Zhong, H., Leung, D. Y. C., and Huang, H.: Harnessing air–water interface to generate interfacial ROS for ultrafast environmental remediation, Nat. Commun., 15, 8860, https://doi.org/10.1038/s41467-024-53289-z, 2024.

Zhang, Q. and Anastasio, C.: Chemistry of fog waters in California's Central Valley—Part 3: concentrations and speciation of organic and inorganic nitrogen, Atmos. Environ., 35 (32), 5629–5643, https://doi.org/10.1016/S1352-2310(01)00337-5, 2001.

Zhang, Y., Yang, X., Gu, J., Liu, Y., Wang, Z., Liu, B., Li, H., and Zhang, X.: H_2O_2-Driven Sulfate Formation at Air–Water Interfaces: Stepwise Mechanism and Accelerated Kinetics, Environ. Sci. Technol., acs.est.5c17902, https://doi.org/10.1021/acs.est.5c17902, 2026.